TFE3-immunopositive papillary renal cell carcinoma: A clinicopathological, immunohistochemical, and genetic study

高松, 大

Pathology - Research and Practice 242 (2023) 154313

Contents lists available at ScienceDirect

Pathology - Research and Practice

journal homepage: www.elsevier.com/locate/prp

TFE3-immunopositive papillary renal cell carcinoma: A clinicopathological, immunohistochemical, and genetic study

Dai Takamatsu [a], Kenichi Kohashi [a], Daisuke Kiyozawa [a], Fumio Kinoshita [a], Kosuke Ieiri [b], Masaya Baba [c], Masatoshi Eto [b], Yoshinao Oda [a,*]

[a] Department of Anatomic Pathology, Graduate School of Medical Sciences, Kyushu University, Higashi-Ku, Fukuoka, Japan
[b] Department of Urology, Graduate School of Medical Sciences, Kyushu University, Higashi-Ku, Fukuoka, Japan
[c] International Research Center for Medical Sciences (IRCMS), Kumamoto University, Kumamoto, Japan

ARTICLE INFO

Keywords:
Papillary renal cell carcinoma
Renal cell carcinoma
TFE3
Whole exome sequence

ABSTRACT

It is possible that PRCCs may still contain a variety of unknown histologic subtypes. Some PRCCs express high expression of TFE3 protein without TFE3 gene rearrangement, but no reports have investigated the significance of this. Here we attempted to examine clinicopathological and molecular significance of the TFE3-immunopositive PRCC. We reviewed the histology and immunohistochemistry in 58 PRCCs. TFE3 immunoexpression was recognized in 7 cases. Because TFE3 immunostaining shows false-positive, to ensure the integrity of TFE3 immunostaining, the immunostaining was performed under strict control of internal controls and western blotting was performed on 2 positive cases and 5 negative cases, and differences in protein expression between two groups were confirmed. Significant immunohistochemical expressions of autophagy/lysosome proteins were observed in TFE3-positive group. No TFE3 gene arrangement was detected in all positive cases by fluorescence *in situ* hybridization. Whole-exome sequencing was performed on 6 TFE3-positive and 2 TFE3-negative cases. Gain of chromosome 7 was found in five of 6 TFE3-positive cases (83%). TFE3-positive group was correlated significantly with higher pTstage, cNstage, WHO/ISUP nuclear grade, and decreased OS. TFE3-immunopositive PRCC group had a poorer prognosis than TFE3-negative PRCC group and showed correlation with expressions of autophagy/lysosome proteins, suggesting that enhancement of autophagy/lysosome function drives an environment of energy metabolism that is favorable for cancer. It is necessary to recognize that there is TFE3-immunopositive group without TFE3 gene rearrangement within PRCC. Because of its aggressive biological behaviour, TFE3 can act as a biomarker in PRCC; moreover, autophagy-inhibiting drugs may have therapeutic effects on TFE3-immunopositive PRCC.

1. Introduction

Renal cell carcinomas are malignant tumors that occur in the kidney and are classified as clear cell RCC, papillary RCC, chromophobe RCC, collecting duct carcinoma, and so on [1]. Recent advances in pathological and molecular biological analysis have revealed subtypes such as MiT family translocation RCC [2–9] and FH-deficient RCC [10–17]. The conventional classification of PRCC into type 1 and type 2 subtypes [18] has been proven difficult to implement [19,20]. Some PRCC histologically overlaps with MiT-translocation RCC and FH-deficient RCC; these three may be difficult to differentiate by morphology alone [21]. In addition, accurate histological and molecular diagnosis and evaluation of malignancy are becoming increasingly important for therapeutic options to improve prognoses.

TFE3 is a member of the helix-loop-helix family of transcription factors. It binds to the μE3 motif of the immunoglobulin heavy-chain enhancer and is expressed in many cell types [22]. In pancreatic adenocarcinoma, TFE3 acts as a transcription-related factor that regulates lysosome biogenesis and autophagy and has been suggested to be related to malignancy [23]. Moreover, since TFE3-related translocations increase TFE3 protein expression, TFE3 protein expression is considered to be one of the useful markers for differential diagnosis. However, the specificity of TFE3 immunohistochemistry has been found to be not perfect [24].

* Correspondence to: Department of Anatomic Pathology, Pathological Sciences, Graduate School of Medical Sciences, Kyushu University, Maidashi 3-1-1, Higashi-Ku, Fukuoka 812-8582, Japan.
E-mail address: oda.yoshinao.389@m.kyushu-u.ac.jp (Y. Oda).

https://doi.org/10.1016/j.prp.2023.154313
Received 13 November 2022; Accepted 14 January 2023
Available online 16 January 2023
0344-0338/

In this study, we investigated the immunohistochemical expression of TFE3 and markers of autophagy/lysosome proteins such as CTSS, ATP6V1H, and ULK2. TFE3 immunohistochemistry was performed under strict control of internal controls and western blotting was demonstrated to confirm the integrity of the TFE3 immunostaining. It is analysed that the relationship between immunohistochemical results and clinicopathological and genetic factors in the TFE3-immunopositive PRCC group.

2. Materials and methods

2.1. Case selection

Paraffin-embedded (FFPE) specimens of surgically resected RCC at Kyushu University Hospital between 1991 and 2018, we retrieved the files of 69 cases diagnosed with PRCC based on the most recent WHO classification [1]. Supplementary Fig. 1 shows the case selection algorithm. First, 7 acquired cystic disease-associated renal cell carcinomas, 2 clear cell papillary renal cell carcinomas, and 1 mucinous tubular and spindle cell carcinoma were excluded by reexamination of their histologies. Next, the remaining cases were immunostained by TFEB, FH, and SMARCB1/INI1, and 1 case of FH-deficient renal cell carcinoma was excluded. Ultimately, formalin-fixed, paraffin-embedded specimens from 58 papillary renal cell carcinoma cases were included; concordant frozen tissue samples of 7 of these cases were also available. The histological review was based on light microscopic examinations with haematoxylin-eosin (HE) staining. Three pathologists (D.T., D.K., and K. K.) independently evaluated the HE and immunohistochemical slides in a blind fashion. Clinical features were collected including age at operation, sex, presence or absence of symptoms, tumor size, surgical treatment, WHO type classification, tumor-node-metastasis (TNM) stage according to the 2017 Union for International Cancer Control TNM staging (T1a-T4, N0–2, and M0 or M1), cancer recurrence and cancer death. The institutional review board at Kyushu University approved this study (IRB number: 2019–108).

2.2. Immunohistochemistry

FFPE tumor tissue sections at 4-μm thickness were used for immunohistochemical staining of CK7, CD10, AMACR, vimentin, HMB45, MelanA, Cathepsin K, TFE3, TFEB, FH, SMARCB1/INI1, CTSS, ATP6V1H, and ULK2. Except for vimentin and HMB45 staining, sections were pretreated by Target Retrieval Solution (MelanA, Cathepsin K, TFE3, SMARCB1/INI1, FH, ATP6V1H, ULK2), polyoxyethylene sorbitan monolaurate (CK7), sodium citrate (CD10, TFEB, CTSS) or ethylenediaminetetraacetic acid (AMACR). The primary monoclonal and polyclonal antibodies used in this study are listed in Supplemental Table 1.

According to a previous study, the immunoreactivity of TFE3 was evaluated in a semiquantitative manner based on both nuclear intensity labelling and the percentage of immunopositive tumor cells [25]. The score was calculated by multiplying the staining intensity (0, no staining; 1, mild staining; 2, moderate staining; and 3, strong staining (Fig. 1)) by the percentage of immunoreactive tumor cells (0−100). The immunostaining result was interpreted as negative when the score was 0–200 and positive when the score was 201–300. The internal positive control of TFE3 was nuclear expression of renal glomerular epithelial cells and negative expression in a renal tubular cell (Supplementary Fig. 2). Tumor cells with cytoplasmic expression were considered negative unless the immunostaining of the nuclei was more intense than that of the cytoplasm [24]. Results of CK7, CD10, AMACR, vimentin, HMB45, MelanA, Cathepsin K, SMARCB1/INI1, TFEB, FH, CTSS, ATP6V1H, and ULK2 were defined based on the tumor proportion score (TPS), and we considered TPS> 50% as positive.

2.3. Cell culture of Xp11 translocation renal cell carcinoma

Human Xp11 translocation renal cell carcinoma cells (RCB4699) were provided by RIKEN BRC Cell Bank. These cells were cultured in Dulbecco's modified Eagle's medium (DMEM; Invitrogen Corp., Carlsbad, CA) supplemented with 10% fetal bovine serum plus penicillin and streptomycin. Cells were grown at 37 °C in a humidified 5% CO_2 incubator.

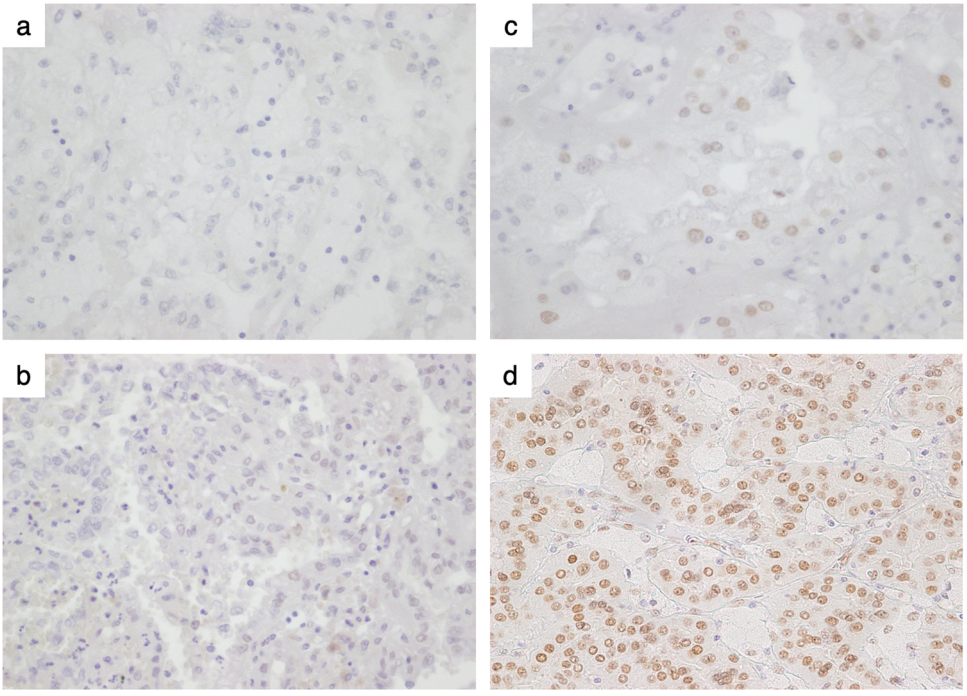

Fig. 1. Representative images of intensity score for TFE3 staining. The score was classified into four levels based on the staining of the nuclei: 0 = no staining (a), 1 = mild (b), 2 = moderate (c), and 3 = strong (d).

2.4. Western blotting

Standard Western blotting was carried out using whole-cell protein lysates and protein lysates obtained from the 7 frozen samples of PRCC, including 2 TFE3-immunopositive and 5 TFE3-negative cases, with a primary antibody against TFE3 (rabbit polyclonal, clone MRQ-37; Sigma Aldrich, USA, 1:4000) and a secondary antibody (anti-rabbit IgG; Cell Signaling). Equal protein sample loading was monitored using an anti-GAPDH antibody (Santa Cruz Biotechnology, sc32233, 1:1000). Protein bands were detected using the ImageQuant LAS 4000 system (GE Healthcare). Quantification was performed using the Fiji (ImageJ) software program (National Institutes of Health).

2.5. TFE3 break-Apart Fluorescence in situ hybridization (FISH) analysis

We performed fluorescence *in situ* hybridization (FISH) on cases that were positive for TFE3 by immunohistochemistry (IHC) to detect *TFE3* gene rearrangement. Break-apart probes for the *TFE3* gene (TFE3 Split Dual Color FISH Probe; GSP Laboratory, Japan) were used. Fluorescence signals were reviewed using a fluorescent microscope (BZ-9000, Keyence, Japan). A TFE3 gene split was indicated by green and red signals separated by a distance of ≥ 2 signal diameters. We counted 100 non-overlapping tumor cells, and TFE3 rearrangement was considered positive if more than 10% of the tumor cells showed TFE3 gene divisions.

2.6. Whole-exome sequencing and data analysis

For genetic comparisons between TFE3-positive and -negative cases, whole-exome sequencing of tumor and non-cancerous kidney tissue DNA was performed by next-generation sequencing. Select cases included 6 TFE3-positive cases and 2 TFE3-negative cases, all of them resected after 2013. Genomic DNAs from tumor and concordant kidneys were separately extracted from 10-μm-thick paraffin-embedded tissue using the solid-phase reversible immobilization (SPRI) method (FormaPure DNA KIT; Beckman Coulter, U.S.) according to the manufacturer's instructions. The quality and quantity of the DNA were evaluated using a Qubit 2.0 Fluorometer. The sequencing library was prepared by random DNA fragmentation and amplification, using SureSelect XT (Agilent Technologies, U.S.). The enriched DNA was sequenced on NovaSeq6000 (Illumina, Inc., U.S.). We commissioned Macrogen Inc. to perform library construction and DNA sequencing. The raw sequence data were evaluated by Fast QC v0.11.9 and trimmed using Trimmomatic v-0.38 by Cell Innovator Inc.

The sequence data were aligned to the hg38 human reference genome by BWA-MEM(BWA 0.7.17). Samtools 1.9 and bcftools 1.9 were used for variant calling. The annotation was performed by VEP (Ensembl database version: 100). Samples with low sequence depth (average depth <30x) were excluded from the subsequent analysis of mutation calls. In order to remove polymorphisms and sequencing errors, those variants having an insufficient number of reads (total reads of tumor <8 and variant reads of tumor <3), a variant allele fraction (VAF) < 20% and normal VAF > 2%, a somatic p-value of < 0.10, or a strand bias (= 0 or 1) were further excluded. For pathway analysis, we used the sets of pathways and genes described in the previous study [26]. Copy number alteration was detected by using a CNV kit 0.9.6. The tumor mutation burden (TMB) and copy number alteration were calculated for each case by Cell Innovator Inc.

2.7. Statistical analysis

JMP Statistical Discovery Software (version 14.0; SAS Institute Inc.) was used for the statistical analyses. Values of $P < 0.05$ were considered to indicate statistical significance. Fisher's exact test was adopted to investigate the relationship between clinicopathological features and the expression of TFE3. Progression-free survival (PFS) was defined as the time from surgery to the date when a new distal metastasis was detected or last follow-up, and overall survival (OS) was defined as the time from surgery to last follow-up or death from RCC. Both PFS and OS were analysed using the Kaplan-Meier method and compared by the Wilcoxon test.

3. Results

3.1. Clinicopathological characteristics and follow-up

The clinical characteristics are summarized in Table 1. The median age was 65 years (range: 39–77 years). Forty-eight male (83%) and 10 female (17%) patients were included. The tumor produced symptoms in 13 patients (22%). The median tumour size was 4.45 cm (range: 1.2–15.5 cm). Radical and partial nephrectomy were performed in 22 cases (38%) and 36 cases (62%), respectively. In the TNM staging, 41 (71%) cases were categorized as pT1a-b, 3 cases (5%) as pT2a-b, and 14 cases (24%) as pT3a-c, but none was categorized as pT4. Regional lymph node metastases developed in 3 cases (5%) and distant metastases in 3 cases (5%). The median recurrence period was 31.5 months (range: 5–184 months), and the median cancer death period was 43 months (range: 11–184 months).

3.2. Immunohistochemical results

Seven of the 58 PRCC cases were positive for TFE3 (Supplemental Table 2). There was no significant difference between TFE3-positive and -negative cases for any of the immunostainings, including CK7, CD10, AMACR, vimentin, HMB45, MelanA, and Cathepsin K (Supplemental Table 3). As for CTSS, ATP6V1H, and ULK2 immunostainings, their expressions were significantly more frequent in TFE3-immunopositive cases ($P = 0.006$, 0.0295, 0.0438, respectively) (Table 2 **and** Fig. 2).

3.3. Western blotting

Two of the 7 cases for which Western blotting was performed were TFE3-immunopositive, and the others were negative. TFE3 protein expression was confirmed in the TFE3-immunopositive cases and the TFE3 cell line, but no TFE3 protein expression was observed in any of the negative cases (Fig. 3). The results of western blotting and immunostaining were in agreement.

Table 1
Clinicopathological summary of the patients.

Clinical features		n = 58
Sex	Male	48 (83%)
	Female	10 (17%)
Age(y)	Median (range)(year)	65 (39–77)
	65y>	28 (48%)
	≧ 65y	30 (52%)
Symptoms	Presence	13 (22%)
	Absence	45 (78%)
Tumor size	Median (range)(cm)	4.45 (1.2–15.5)
Treatment	Partial	22 (38%)
	Radical	36 (62%)
cT stage	cT1a-b	41 (71%)
	cT2a-b	3 (5%)
	cT3a-c	14 (24%)
	cT4	0 (0%)
cN stage	cN0	55 (95%)
	cN1–2	3 (5%)
cM stage	cM0	55 (95%)
	cM1	3 (5%)
Recurrence	+ /-	15/40 (27.8%)
	Median (range) (month)	8 (5–71)
Cancer death	+ /-	13/41 (24%)
	Median (range) (month)	43 (11–111)

Table 2
Comparison of the expression of CTSS, ATP6V1H and ULK2 according to TFE3 expression.

		TFE3 (+) (n = 7)	TFE3 (-) (n = 51)	*P*-value
CTSS	+	4 (57.1%)	7 (13.7%)	0.006*
	-	3 (42.9%)	44 (86.3%)	
ATP6V1H	+	4 (57.1%)	10 (19.6%)	0.0295*
	-	3 (42.9%)	41 (80.4%)	
ULK-2	+	4 (57.1%)	11 (21.6%)	0.0438*
	-	3 (42.9%)	40 (78.4%)	

* Significant difference.

3.4. FISH analysis of TFE3 gene rearrangement

TFE3 break-apart FISH analysis was performed for all TFE3-positive cases. None of the positive cases in the study was female. No TFE3 gene rearrangement was detected (Supplementary Fig. 3). Additionally, no *TFE3* amplification was detected.

3.5. Genetic comparative analysis between positive and negative cases

When we compared the TFE3-positive and -negative cases by key pathways, following a previous study [26], a hot-spot mutation of the *MET* gene (*p.M1268T*) was found in 1 positive case, and a gain of chromosome 7 in 5 positive cases (Fig. 4). Furthermore, a mutation of one of the chromatin modifiers (*KDM4B, KDM6B, SMYD4,* or *KMT2B*) was observed in 1 case each, but no mutations in the Hippo pathway or SWI/SNF complex were observed. There were no recurrent or common somatic mutations in any case. and no mutations were observed in the peripheral genes related to TFE3, including *FLCN, PGC1α/β, FNIP, GSK3β,* or *calcineurin*. The tumor mutation burden was not significantly different between the positive and negative groups ($P = 0.0874$).

3.6. Clinicopathological and morphological features of TFE3-positive cases

The clinicopathological and morphological features of TFE3-positive cases are summarized in Table 3. There were no females among the TFE3-positive cases. Four patients were diagnosed with advanced local disease stage (≧pT3) ($P = 0.0437$), and 2 patients developed metastasis of regional lymph nodes (cN1 or cN2) ($P = 0.0358$). All cases had WHO/ISUP nuclear grade 3 ($P = 0.0134$). Clinicopathologically and morphologically, there was no significant difference in any other factor.

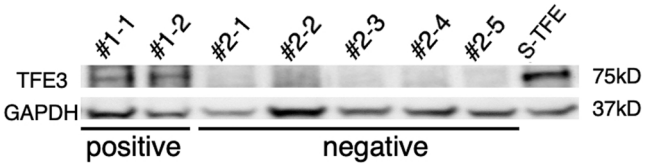

Fig. 3. Comparison of TFE3 protein expression between the TFE3-positive and TFE3-negative groups. From left to right, the columns show results for the TFE3-positive group (#1–1,#1–2), the TFE3-negative group (#2–1, #2–2, #2–3, #2–4, #2–5), and the TFE3-rearranged renal cell carcinoma cell line (S-TFE). TFE3 protein expression was confirmed in the TFE3 cell line and the TFE3-positive group, but no TFE3 protein expression was observed in any cases in the TFE3-negative group.

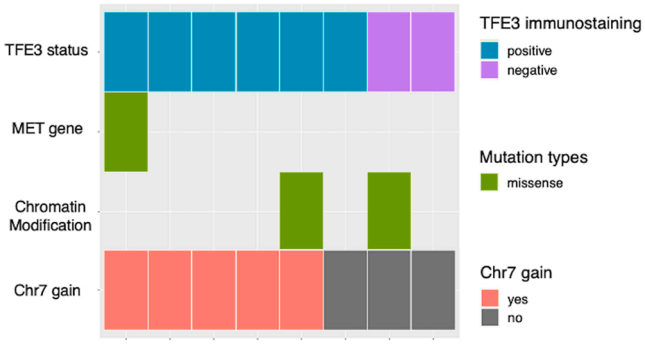

Fig. 4. Analysis of whole-exome sequencing between the TFE3 -positive and -negative groups. There were no recurrent or common somatic mutations in any case. When we compared the TFE3-positive and negative groups by key pathways, following a previous study, a hot-spot mutation of the MET gene (p.M1268T) was found in 1 TFE3-positive case, and a gain of chr7 was observed in 5 of the 6 cases of the TFE3-negative group. Pathways and genes represented include *MET*, the Hippo pathway (NF2, SAV1, and WWC1), the NRF2 pathway (NFE2L2, KEAP1, CUL3, SIRT1, and FH), chromatin modification (CREBBP, DOTL1, EHMT1/2, EP300, EZH1/2, KAT2A/B, KDM1A/B, KDM4A/B, KDM5A/B/C, KDM6A/B, MLL1/2/3/4/5, NSD1, SETD2, SMYD4, and SRCAP), the SWI/SNF complex (ACTB, ACTL6A/B, ARID1A/B, ARID2, BCL6A/B/C, BCL11A/B, BRD7/9, DPF1/2/3, PHF10, PBRM1, SMARCA2/4, SMARCB1, SMARCC1/2, SMARCD1/2/3, and SMARCE1), the mammalian target of rapamycin (mTOR) pathway (MTOR, PIK3CA, PTEN, STK11, TSC1, and TSC2), and the p53 pathway (ATM, CDKN1A, CDKN2A, FBXW7, RB1, and TP53).

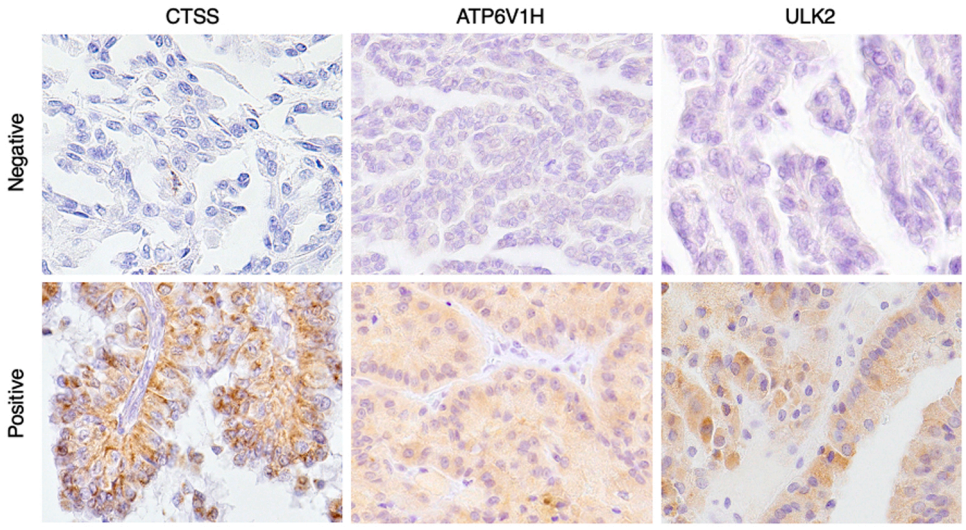

Fig. 2. Representative images of immunohistochemistry of autophagy and lysosomal proteins. Immunohistochemistry showed upregulation of the proteins in the TFE3-positive compared with the TFE3-negative groups.

Table 3
Association between TFE3 expression and clinicopathological factors.

Factors		positive	negative	*P*-value
		(n = 7)	(n = 51)	
Age (Median)		67 (39–74)	64 (39–77)	0.7743
Sex	M	7 (12.0%)	41 (70.8%)	0.3356
	F	0 (0%)	10 (17.2%)	
Tumor size (Median)		4 (1.6–11.5)	4.5 (1.2–15.5)	0.6785
pT stage	T1–2	3 (5.2%)	41 (70.7%)	0.0437*
	T3–4	4 (6.9%)	10 (17.2%)	
cN stage	N0	5 (8.6%)	50 (86.2%)	0.0358*
	N1–2	2 (3.5%)	1 (1.7%)	
cM stage	M0	6 (10.3%)	49 (84.5%)	0.3251
	M1	1 (1.7%)	2 (3.5%)	
WHO/ISUP grade	1/2	0 (0%)	26 (44.8%)	0.0134*
	3/4	7 (12.1%)	25 (43.1%)	
Sarcomatoid		0 (0%)	2 (3.5%)	1
Foamy histiocytes		5 (8.6%)	23 (40.0%)	0.2458
Cholesterol clefts		2 (3.5%)	12 (20.7%)	1
Necrosis		3 (5.2%)	17 (29.3%)	0.6828

* Significant difference.

3.7. Survival analysis

TFE3-positive cases tended to show a worse progression-free survival ($P = 0.0635$, Fig. 5**a**) and had a significantly worse overall survival ($P = 0.0326$, Fig. 5**b**).

4. Discussion

Traditionally, PRCC has been classified as type 1 and type 2 [18], but this classification is not currently recommended for several reasons [19,20,27]. Some previously unrecognized but distinctive types of carcinomas, including MiT family translocation RCC and FH-deficient RCC, have been found in a group of tumors previously classified as “type 2 PRCC” [21]. It is now recognized that WHO/ISUP grade and tumor architecture, including specific morphologic patterns, rather than the classic tumor types, better predict outcomes [28]. In this study, we also re-examined the histology and immunohistochemistry of cases originally diagnosed with PRCC and excluded 11 of the 69 cases as different diagnoses.

In general, specific histologic features associated with a poorer prognosis include WHO/ISUP nuclear grade, stage, microvascular invasion, absence of foam cells, and sarcomatoid transformation in PRCC [29,30]. Significant differences in WHO/ISUP nuclear grade, pTstage, and cNstage were also observed in this study.

This study demonstrated a correlation between TFE3 immunoexpression and overall survival in PRCC. It has been reported that increased TFE3 expression in RCC was associated with poor PFS regardless of the gene translocation status [31]. The TFE3 protein has been proven to be required for tumor growth in pancreatic ductal adenocarcinoma (PDA), one of the cancers with the worst prognosis [23]. Therefore, it is suggested that TFE3 may be useful as a prognostic marker.

The activation of cellular stress response pathways to maintain metabolic homeostasis is considered a critical growth and survival mechanism in many cancers [32]. Autophagy is an evolutionarily conserved, intracellular self-defence mechanism that relieves cells of the harmful accumulation of damaged or unwanted components and allows recycling of these components to maintain metabolic homeostasis [15,33]. Enhanced autophagy is a mechanism of resistance for cancer cells faced with metabolic and therapeutic stress [34]. TFE3 is a nutrient-responsive transcription factor that promotes energy metabolism such as autophagy and lysosome biogenesis, and is triggered by the nuclear translocation of TFE3 proteins [35]. Pathways and cellular processes regulated by MiT/TFE factors include autophagy and lysosomal biogenesis [36]. In pancreatic ductal adenocarcinoma (PDA), immunohistochemistry has shown increased upregulation of autophagy-lysosome proteins in the tumor epithelium compared to normal pancreatic tissue, and there is evidence at the cellular level that TFE3 is associated with tumor growth [23]. The current study shows that autophagy-lysosome protein-related staining correlates with TFE3 staining and poorer prognosis, indicating the existence of a similar mechanism as in PDA.

Immunohistochemistry to detect TFE3 translocation is simple, fast and inexpensive, but FISH is the gold standard test [37–40]. The sensitivity of TFE3 immunohistochemistry is considered high, but its specificity is not perfect [24], and some RCCs express TFE3 but do not harbour a translocation [31]. Therefore, TFE3 immunohistochemistry must be performed under strict conditions. In this study, TFE3 immunohistochemistry was performed under strict control of internal controls and western blotting was used to demonstrate the difference in protein

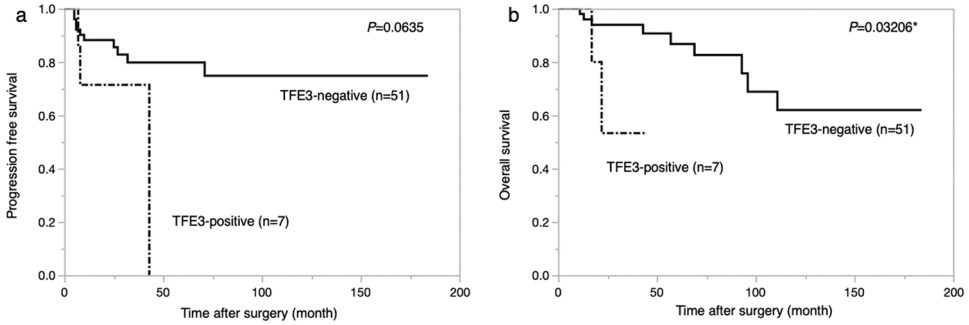

Fig. 5. Kaplan-Meier curves of progression-free survival and overall survival according to TFE3 immunostaining. TFE3-positive cases were related to a worse trend of progression-free survival ($P = 0.0635$, **a**) and significantly worse overall survival ($P = 0.0326$, **b**).

expression between TFE3 immunopositive and -negative cases to confirm the integrity of TFE3 immunostaining. Some PRCC is diffusely positive for TFE3 immunostaining, similar to MiT family translocation RCC. These results reaffirm the need for FISH for accurate diagnosis, even if carcinoma cells are diffusely positive for TFE3.

Type 1 PRCC frequently develops gains in chromosomes 7 and 17, while Type 2 PRCC has a more heterogenous profile with an allelic imbalance of one or more chromosomes [30]. Comprehensive molecular characterization of 161 primary PRCCs revealed that Type 1 PRCC was associated with MET alterations, whereas Type 2 PRCC was characterized by CDKN2A silencing, SETD2 mutations, and TFE3 fusions, increased expression of the NRF2-antioxidant response element pathway, and CpG island methylator phenotype [26]. These previous findings indicate that PRCC is a group with diverse genetic abnormalities.

To investigate the reason for the high expression of TFE3 without TFE3 gene rearrangement, whole-exome sequencing was performed on 6 TFE3-positive and 2 TFE3-negative cases. The results showed no differences in the number or type of gene mutations in the pathways and peripheral genes related to TFE3, including FLCN, PGC1α/β, FNIP, GSK3β, and calcineurin, indicating that there was no significant difference in tumor mutation burden between the positive and negative groups. Since we were unable to attribute the mechanism of high TFE3 expression without TFE3 rearrangement to a genetic abnormality, we speculate that this mechanism may have involved epigenetic changes. Somatic mutation of MET or the gain of chromosome 7, which encodes MET, was recurrently observed in TFE3-positive PRCC. This mutational background is similar to type 1 PRCC. Interestingly, there were no positive cases of tumors with morphologic features similar to those of type 1 PRCC.

In conclusion, among 58 cases of PRCC surgically resected at our institution, we found that there was a TFE3-immunopositive group without TFE3 gene rearrangement. FISH is needed to rule out Xp11.2 TRCC for the diagnosis of TFE3-immunopositive PRCC. TFE3 overexpression correlated significantly with autophagy/lysosome proteins and a poor prognosis. TFE3 should be considered as a surrogate marker in PRCC, and autophagy inhibitors may have therapeutic effects on TFE3-immunopositive PRCC.

Funding

This study was supported by JSPS KAKENHI Grant Number 19H03444.

Compliance with ethical standards

This study was conducted in accordance with the principles embodied in the Declaration of Helsinki. The study was approved by the institutional review board at Kyushu University (IRB number: 2019–108).

CRediT authorship contribution statement

D. Takamatsu performed the research and wrote the paper. K. Kohashi, D. Kiyozawa, F. Kinoshita, K. Ieiri, and M. Baba contributed to the research design and slide review. M. Eto and Y. Oda designed the research and gave final approval of the manuscript. All authors critically reviewed and approved the manuscript.

Acknowledgments

Technical support for the experimental trials was provided by the following laboratory assistants: Motoko Tomita, Mami Nakamizo, Juri Godo, Kozue Ueno-Matsuda, Miwako Ishii, Jumi Yahiro-Matsumoto, and Haruka Inoue. We also appreciate the technical assistance from The Research Support Center, Kyushu University Graduate School of Medical Sciences. The English used in this manuscript was revised by KN International (http://www.kninter.com/).

Conflicts of interest/Disclosure

All authors declare that have no conflicts of interest to disclose.

Appendix A. Supporting information

Supplementary data associated with this article can be found in the online version at doi:10.1016/j.prp.2023.154313.

References

[1] M.B. Amin, et al., Papillary renal cell carcinoma. The WHO classificaion of tumours editorial board eds. WHO classification of tumours: 5th edition. Urinary and Male Genital Tumours, IARC Press, Lyon, France, 2022.
[2] J. Pei, H. Cooper, D.B. Flieder, J.N. Talarchek, T. Al-Saleem, R.G. Uzzo, E. Dulaimi, A.S. Patchefsky, J.R. Testa, S. Wei, NEAT1-TFE3 and KAT6A-TFE3 renal cell carcinomas, new members of MiT family translocation renal cell carcinoma, Mod. Pathol. 32 (2019) 710–716.
[3] H. Fukuda, I. Kato, M. Furuya, R. Tanaka, T. Takagi, T. Kondo, Y. Nagashima, A novel partner of TFE3 in the Xp11 translocation renal cell carcinoma: clinicopathological analyses and detection of EWSR1-TFE3 fusion, Virchows Arch. 474 (2019) 389–393.
[4] G. Martignoni, S. Gobbo, P. Camparo, M. Brunelli, E. Munari, D. Segala, M. Pea, F. Bonetti, P.B. Illei, G.J. Netto, M. Ladanyi, M. Chilosi, P. Argani, Differential expression of cathepsin K in neoplasms harboring TFE3 gene fusions, Mod. Pathol. 24 (2011) 1313–1319.
[5] J. Marcon, R.G. DiNatale, A. Sanchez, R.R. Kotecha, S. Gupta, F. Kuo, V. Makarov, A. Sandhu, R. Mano, A.W. Silagy, et al., Comprehensive genomic analysis of translocation renal cell carcinoma reveals copy-number variations as drivers of disease progression, Clin. Cancer Res. 26 (2020) 3629–3640.
[6] J. Clark, Y.J. Lu, S.K. Sidhar, C. Parker, S. Gill, D. Smedley, R. Hamoudi, W. M. Linehan, J. Shipley, C.S. Cooper, Fusion of splicing factor genes PSF and NonO (p54nrb) to the TFE3 gene in papillary renal cell carcinoma, Oncogene 15 (1997) 2233–2239.
[7] M. Ladanyi, M.Y. Lui, C.R. Antonescu, A. Krause-Boehm, A. Meindl, P. Argani, J. H. Healey, T. Ueda, H. Yoshikawa, A. Meloni-Ehrig, P.H. Sorensen, F. Mertens, N. Mandahl, H. van den Berghe, R. Sciot, P. Dal Cin, J. Bridge, The der(17)t(X;17)(p11;q25) of human alveolar soft part sarcoma fuses the TFE3 transcription factor gene to ASPL, a novel gene at 17q25, Oncogene 20 (2001) 48–57.
[8] Q.Y. Xia, X.T. Wang, X.M. Zhan, X. Tan, H. Chen, Y. Liu, S.S. Shi, X. Wang, X. Wei, S.B. Ye, R. Li, H.H. Ma, Z.F. Lu, X.J. Zhou, Q. Rao, Xp11 translocation Renal Cell Carcinomas (RCCs) with RBM10-TFE3 gene fusion demonstrating melanotic features and overlapping morphology with t(6;11) RCC: interest and diagnostic pitfall in detecting a paracentric inversion of TFE3, Am. J. Surg. Pathol. 41 (2017) 663–676.
[9] K. Pivovarcikova, P. Grossmann, R. Alaghehbandan, M. Sperga, M. Michal, O. Hes, TFE3-Fusion variant analysis defines specific clinicopathologic associations amog Xp11 translocation cancers, Am. J. Surg. Pathol. 41 (2017) 138–140.
[10] G. Sun, X. Zhang, J. Liang, X. Pan, S. Zhu, Z. Liu, C.M. Armstrong, J. Chen, W. Lin, B. Liao, T. Lin, R. Huang, M. Zhang, L. Zheng, et al., Integrated molecular characterization of fumarate hydratase-deficient renal cell carcinoma, Clin. Cancer Res. 27 (2021) 1734–1743.
[11] J.P. Gleeson, I. Nikolovski, R. Dinatale, M. Zucker, A. Knezevic, S. Patil, Y. Ged, R. R. Kotecha, N. Shapnik, S. Murray, P. Russo, J. Coleman, C.H. Lee, Z.K. Stadler, A. A. Hakimi, D.R. Feldman, R.J. Motzer, E. Reznik, M.H. Voss, Y.B. Chen, M.I. Carlo, Comprehensive molecular characterization and response to therapy in fumarate hydratase-deficient renal cell carcinoma, Clin. Cancer Res. 27 (2021) 2910–2919.
[12] M. Muller, M. Guillaud-Bataille, J. Salleron, C. Genestie, S. Deveaux, A. Slama, B. B. de Paillerets, S. Richard, P.R. Benusiglio, S. Ferlicot, Pattern multiplicity and fumarate hydratase (FH)/S-(2-succino)-cysteine (2SC) staining but not eosinophilic nucleoli with perinucleolar halos differentiate hereditary leiomyomatosis and renal cell carcinoma-associated renal cell carcinomas from kidney tumors without FH gene alteration, Mod. Pathol. 31 (2018) 974–983.
[13] S.C. Smith, K. Trpkov, Y.B. Chen, R. Mehra, D. Sirohi, C. Ohe, A.K. Cani, D. H. Hovelson, K. Omata, J.B. McHugh, W. Jochum, M. Colecchia, M. Amin, et al., Tubulocystic carcinoma of the kidney with poorly differentiated foci: a frequent morphologic pattern of fumarate hydratase-deficient renal cell carcinoma, Am. J. Surg. Pathol. 40 (2016) 1457–1472.
[14] S.R. Williamson, A.J. Gill, P. Argani, Y.B. Chen, L. Egevad, G. Kristiansen, D. J. Grignon, O. Hes, Report from the International Society of Urological Pathology (ISUP) consultation conference on molecular pathology of urogenital cancers: III: molecular pathology of kidney cancer, Am. J. Surg. Pathol. 44 (2020) e47–e65.
[15] Y.B. Chen, A.R. Brannon, A. Toubaji, M.E. Dudas, H.H. Won, H.A. Al-Ahmadie, S. W. Fine, A. Gopalan, N. Frizzell, M.H. Voss, P. Russo, M.F. Berger, S.K. Tickoo, V. E. Reuter, Hereditary leiomyomatosis and renal cell carcinoma syndrome-associated renal cancer: recognition of the syndrome by pathologic features and the utility of detecting aberrant succination by immunohistochemistry, Am. J. Surg. Pathol. 38 (2014) 627–637.

[16] K. Trpkov, O. Hes, A. Agaimy, M. Bonert, P. Martinek, C. Magi-Galluzzi, G. Kristiansen, C. Luders, G. Nesi, E. Comperat, M. Sibony, D.M. Berney, R. Mehra, F. Brimo, A. Hartmann, A. Husain, N. Frizzell, K. Hills, F. Maclean, B. Srinivasan, A. J. Gill, Fumarate hydratase-deficient renal cell carcinoma is strongly correlated with fumarate hydratase mutation and hereditary leiomyomatosis and renal cell carcinoma syndrome, Am. J. Surg. Pathol. 40 (2016) 865–875.
[17] H.D. Lau, E. Chan, A.C. Fan, C.A. Kunder, S.R. Williamson, M. Zhou, M.T. Idrees, F. M. Maclean, A.J. Gill, C.S. Kao, A clinicopathologic and molecular analysis of fumarate hydratase-deficient renal cell carcinoma in 32 patients, Am. J. Surg. Pathol. 44 (2020) 98–110.
[18] B. Delahunt, J.N. Eble, M.R. McCredie, P.B. Bethwaite, J.H. Stewart, A.M. Bilous, Morphologic typing of papillary renal cell carcinoma: comparison of growth kinetics and patient survival in 66 cases, Hum. Pathol. 32 (2001) 590–595.
[19] R.M. Saleeb, F. Brimo, M. Farag, A. Rompré-Brodeur, F. Rotondo, V. Beharry, S. Wala, P. Plant, M.R. Downes, K. Pace, A. Evans, G. Bjarnason, J.M.S. Bartlett, G. M. Yousef, Toward biological subtyping of papillary renal cell carcinoma with clinical implications through histologic, immunohistochemical, and molecular analysis, Am. J. Surg. Pathol. 41 (2017) 1618–1629.
[20] R.M. Saleeb, P. Plant, E. Tawedrous, A. Krizova, F. Brimo, A.J. Evans, S.J. Wala, J. Bartlett, Q. Ding, D. Boles, F. Rotando, M. Farag, G.M. Yousef, Integrated phenotypic/genotypic analysis of papillary renal cell carcinoma subtypes: identification of prognostic markers, cancer-related pathways, and implications for therapy, Eur. Urol. Focus 4 (2018) 740–748.
[21] K. Trpkov, O. Hes, S.R. Williamson, A.J. Adeniran, A. Agaimy, R. Alaghehbandan, M.B. Amin, P. Argani, Y.B. Chen, L. Cheng, et al., New developments in existing WHO entities and evolving molecular concepts: the Genitourinary Pathology Society (GUPS) update on renal neoplasia, Mod. Pathol. 34 (2021) 1392–1424.
[22] P.S. Henthorn, C.C. Stewart, T. Kadesch, J.M. Puck, The gene encoding human TFE3, a transcription factor that binds the immunoglobulin heavy-chain enhancer, maps to Xp11.22, Genomics 11 (1991) 374–378.
[23] R.M. Perera, S. Stoykova, B.N. Nicolay, K.N. Ross, J. Fitamant, M. Boukhali, J. Lengrand, V. Deshpande, M.K. Selig, C.R. Ferrone, J. Settleman, G. Stephanopoulos, N.J. Dyson, R. Zoncu, S. Ramaswamy, W. Haas, N. Bardeesy, Transcriptional control of autophagy-lysosome function drives pancreatic cancer metabolism, Nature 524 (2015) 361–365.
[24] P. Argani, P. Lal, B. Hutchinson, M.Y. Lui, V.E. Reuter, M. Ladanyi, Aberrant nuclear immunoreactivity for TFE3 in neoplasms with TFE3 gene fusions: a sensitive and specific immunohistochemical assay, Am. J. Surg. Pathol. 27 (2003) 750–761.
[25] B. Yang, H. Duan, W. Cao, Y. Guo, Y. Liu, L. Sun, J. Zhang, Y. Sun, Y. Ma, Xp11 translocation renal cell carcinoma and clear cell renal cell carcinoma with TFE3 strong positive immunostaining: morphology, immunohistochemistry, and FISH analysis, Mod. Pathol. 32 (2019) 1521–1535.
[26] Cancer Genome Atlas Research, W.M. Linehan, P.T. Spellman, C.J. Ricketts, C. J. Creighton, S.S. Fei, C. Davis, D.A. Wheeler, B.A. Murray, L. Schmidt, et al., Comprehensive molecular characterization of papillary renal-cell carcinoma, N. Engl. J. Med. 374 (2016) 135–145.
[27] M. Chevarie-Davis, Y. Riazalhosseini, M. Arseneault, A. Aprikian, W. Kassouf, S. Tanguay, M. Latour, F. Brimo, The morphologic and immunohistochemical spectrum of papillary renal cell carcinoma: study including 132 cases with pure type 1 and type 2 morphology as well as tumors with overlapping features, Am. J. Surg. Pathol. 38 (2014) 887–894.
[28] C. Yang, B. Shuch, H. Kluger, P.A. Humphrey, A.J. Adeniran, High WHO/ISUP grade and unfavorable architecture, rather than typing of papillary renal cell carcinoma, may be associated with worse prognosis, Am. J. Surg. Pathol. 44 (2020) 582–593.
[29] G.P. Paner, V. Chumbalkar, R. Montironi, H. Moch, M.B. Amin, Updates in grading of renal cell carcinomas beyond clear cell renal cell carcinoma and papillary renal cell carcinoma, Adv. Anat. Pathol. 29 (2022) 117–130.
[30] N. Mendhiratta, P. Muraki, A.E. Sisk, B. Shuch Jr., Papillary renal cell carcinoma: review, Urol. Oncol. 39 (2021) 327–337.
[31] H.J. Lee, D.H. Shin, S.Y. Kim, C.S. Hwang, J.H. Lee, W.Y. Park, K.U. Choi, J.Y. Kim, C.H. Lee, M.Y. Sol, S.H. Rha, S.W. Park, TFE3 translocation and protein expression in renal cell carcinoma are correlated with poor prognosis, Histopathology 73 (2018) 758–766.
[32] E. White, Exploiting the bad eating habits of Ras-driven cancers, Genes Dev. 27 (2013) 2065–2071.
[33] R. Amaravadi, A.C. Kimmelman, E. White, Recent insights into the function of autophagy in cancer, Genes Dev. 30 (2016) 1913–1930.
[34] N. Chen, V. Karantza, Autophagy as a therapeutic target in cancer, Cancer Biol. Ther. 11 (2011) 157–168.
[35] J.A. Martina, H.I. Diab, L. Lishu, A.L. Jeong, S. Patange, N. Raben, R. Puertollano, The nutrient-responsive transcription factor TFE3 promotes autophagy, lysosomal biogenesis, and clearance of cellular debris, Sci. Signal 7 (2014) ra9.
[36] R.M. Perera, C. Di Malta, A. Ballabio, MiT/TFE family of transcription factors, lysosomes, and cancer, Annu Rev. Cancer Biol. 3 (2019) 203–222.
[37] Q. Rao, S.R. Williamson, S. Zhang, J.N. Eble, D.J. Grignon, M. Wang, X.J. Zhou, W. Huan, P.H. Tan, G.T. Maclennan, L. Cheng, TFE3 break-apart FISH has a higher sensitivity for Xp11.2 translocation-associated renal cell carcinoma compared with TFE3 or cathepsin K immunohistochemical staining alone: expanding the morphologic spectrum, Am. J. Surg. Pathol. 37 (2013) 804–815.
[38] W.M. Green, R. Yonescu, L. Morsberger, K. Morris, G.J. Netto, J.I. Epstein, P. B. Illei, M. Allaf, M. Ladanyi, C.A. Griffin, P. Argani, Utilization of a TFE3 break-apart FISH assay in a renal tumor consultation service, Am. J. Surg. Pathol. 37 (2013) 1150–1163.
[39] M. Zhong, P. De Angelo, L. Osborne, M. Keane-Tarchichi, M. Goldfischer, L. Edelmann, Y. Yang, W.M. Linehan, M.J. Merino, S. Aisner, M. Hameed, Dual-color, break-apart FISH assay on paraffin-embedded tissues as an adjunct to diagnosis of Xp11 translocation renal cell carcinoma and alveolar soft part sarcoma, Am. J. Surg. Pathol. 34 (2010) 757–766.
[40] J.M. Mosquera, P. Dal Cin, K.D. Mertz, S. Perner, I.J. Davis, D.E. Fisher, M. A. Rubin, M.S. Hirsch, Validation of a TFE3 break-apart FISH assay for Xp11.2 translocation renal cell carcinomas, Diagn. Mol. Pathol. 20 (2011) 129–137.